The mixed-valence state of Ce in the hexagonal $CeNi_4B$ compound

2003 J. Phys.: Condens. Matter 15 1397

(http://iopscience.iop.org/0953-8984/15/9/303)

INSTITUTE OF PHYSICS PUBLISHING JOURNAL OF PHYSICS: CONDENSED MATTER

J. Phys.: Condens. Matter **15** (2003) 1397–1403 PII: S0953-8984(03)54304-1

The mixed-valence state of Ce in the hexagonal $CeNi_4B$ compound

T Toliński[1], A Kowalczyk[1], M Pugaczowa-Michalska[1] and G Chełkowska[2]

[1] Institute of Molecular Physics, Polish Academy of Sciences, Smoluchowskiego 17, 60-179 Poznań, Poland
[2] Institute of Physics, Silesian University, Uniwersytecka 4, 40-007 Katowice, Poland

E-mail: tomtol@ifmpan.poznan.pl

Received 3 October 2002
Published 24 February 2003
Online at stacks.iop.org/JPhysCM/15/1397

Abstract

Measurements of the magnetic susceptibility χ, x-ray photoemission spectra (XPS), electrical resistivity ρ and electronic structure calculations for $CeNi_4B$ are reported. In the paramagnetic region, $CeNi_4B$ follows the Curie–Weiss law with $\mu_{\mathrm{eff}} = 0.52\ \mu_B$/fu and $\theta = -10.7$ K. The effective magnetic moment is lower than the free Ce^{3+}-ion value. The Ce(3d) XPS spectra have confirmed the mixed-valence state of Ce ions in $CeNi_4B$. The f occupancy, n_f, and the coupling Δ between the f level and the conduction states were derived to be about 0.83 and 85 meV, respectively. Both susceptibility data and XPS spectra show that Ce ions in $CeNi_4B$ are in the intermediate-valence state. At low temperatures (below 12 K), the magnetic contribution to the electrical resistivity reveals a logarithmic slope characteristic of Kondo-like systems.

1. Introduction

Despite the increased interest in metallic systems with electronic instability of 4f states known as systems with intermediate valence, heavy fermions and Kondo lattices, the nature of the 4f states of Ce in the phases considered is still unclear at the microscopic level.

The series RNi_4B, where R stands for a rare-earth element or Y, is attracting attention owing to its interesting magnetic, structural and electronic behaviour. The materials belonging to the RNi_4B series create a hexagonal structure of $CeCo_4B$ with space group $P6/mmm$. The Ni atoms occupy the crystallographic sites (2c) and (6c), the rare earth is also located in two sites ((1a), (1b)) and the boron atoms are located in the (2d) positions.

The question of the filling of the Ni(3d) states, i.e., the existence or absence of a magnetic moment on the Ni atoms, is not entirely settled [1–3] for RNi_4B. This question was addressed

in our previous experimental and theoretical x-ray photoemission spectroscopy (XPS) studies. The magnetic properties of the RNi_4B series were also studied in detail [4–6].

The structure of $CeNi_4B$ is consistent with $CeNi_5$, which crystallizes in the hexagonal $CaCu_5$ type of structure. $CeNi_5$ is a paramagnet at all temperatures; its magnetic susceptibility, which is almost isotropic, shows a broad maximum around 100 K [7]. The maximum of the bulk susceptibility in $CeNi_5$ corresponds to Ni atoms. The maximum arises from the thermal smearing of the Ni(3d) electron density of states (DOS) at the Fermi level, enhanced by the spin fluctuations. The presence of the spin fluctuations in $CeNi_5$ was also inferred from the T^2-behaviour of the resistivity and the magnetic susceptibility at low temperature [8]. The behaviour of $CeNi_5$ indicates that in this compound the cerium atom is in the non-magnetic Ce^{4+} ($4f^0$, $J = 0$) state and that the Ni(3d) band is filled.

XPS has become a widely used technique for studies of both the mixed-valence state and the valence bands in rare-earth–transition metal compounds. This method, correlated with magnetic measurements, provides information regarding: the f occupancy, n_f; the coupling, Δ, between the 4f level and the conduction states; and the degree of localization.

In this letter we present magnetic, electronic and electrical resistivity studies of the hexagonal $CeNi_4B$ compound.

2. Experimental details

The $CeNi_4B$ compound was prepared by the induction melting of stoichiometric amounts of the constituent elements in a water-cooled boat, under an argon atmosphere. The crystal structure was established by a powder x-ray diffraction technique, using Cu Kα radiation. The $CeNi_4B$ compound was a single-phase material with a hexagonal structure and the lattice constants $a = 5.002$ Å and $c = 6.988$ Å [4].

The x-ray photoemission spectra were obtained for irradiation with photon energy equal to 1487.6 eV, with a Al Kα source, using a PHI 5700/660 Physical Electronics Spectrometer. The energy spectra of the electrons were analysed by a hemispherical mirror analyser with an energy resolution of about 0.3 eV. The Fermi level $E_F = 0$ was referred to the gold 4f-level binding energy at 84 eV. All photoemission spectra were measured immediately after breaking the sample in a vacuum of 10^{-10} Torr.

The electronic structure and the magnetic moment were calculated by the spin-polarized tight-binding linear muffin-tin orbital (TB LMTO) method in the atomic sphere approximation (ASA) [9]. The self-consistent spin-polarized band calculations were performed for the experimental lattice parameters. The values of the atomic sphere radii were taken in such a way that the sum of all atomic sphere volumes was equal to the volume of the unit cell. In our case the unit cell contains two formula units ($N = 12$ atoms). The exchange–correlation potential was assumed in the form proposed by von Barth and Hedin [10] and Langreth–Mehl–Hu non-local corrections were included [11]. The scalar relativistic wave equation was solved. In the band calculations the initial atomic configurations were taken according to the periodic table of elements. We assume for Ce: core(Xe) + $4f^1 5d^1 6s^2$; for Ni: core(Ar) + $3d^8 4s^2$; and for B: core(He) + $2s^2 2p^1$. Thus, the 4f states of Ce were treated as band ones. Computations were done for 750 k-points in the irreducible wedge of the first Brillouin zone. The tetrahedron method [12] was used for integration over the Brillouin zone. The iterations were repeated until the energy eigenvalues of the consecutive iteration steps were the same within an error of 0.01 mRyd.

Electrical resistivity measurements were carried out by a standard four-probe technique in the temperature range from 4.2 K up to room temperature.

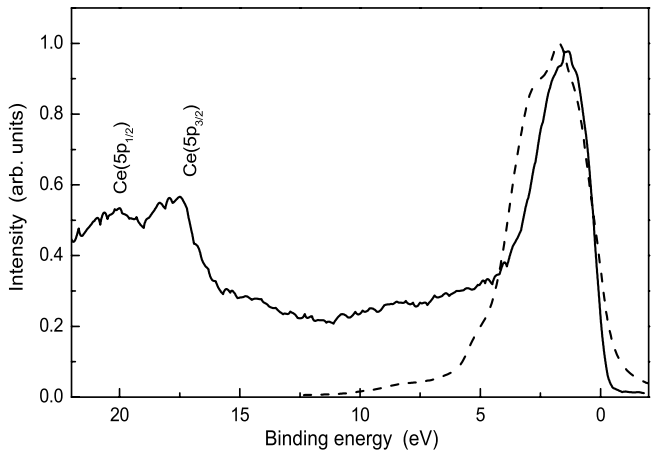

Figure 1. Experimental (solid curve) and calculated (dashed curve) valence band regions of the $CeNi_4B$ compound.

3. Results and discussion

In the Ce-based compounds, depending on the position of the Fermi level E_F compared to that of the 4f state, the following electronic states of cerium are expected: magnetic 3+ state; 3+ state with Kondo effect; and (3+/4+) intermediate-valence state. The cerium–transition metal compounds are attractive for studies of these diverse Ce states because of the strong dependence of the Fermi-level position on the amounts of the contributing elements. The behaviour of Ce changes in various Ce–Ni systems also due to the different crystallographic structures.

The magnetic moment of $CeNi_4B$ measured as a function of an external magnetic field reveals a small curvature, which can be explained by the presence of a small magnetic moment on the Ni atoms [4]. The magnetic moment of $CeNi_4B$ was measured in a magnetic field of 5 T and the resulting dc susceptibility $\chi(T)$ was fitted with a modified Curie–Weiss law $\chi(T) = \chi_0 + C/(T - \theta)$ giving $\chi_0 = 16.6 \times 10^{-9}$ m^3 kg^{-1}, $\theta = -10.7$ K and $C = 11 \times 10^{-7}$ m^3 K kg^{-1} [4]. The effective magnetic moment $\mu_{\text{eff}} = 0.52\ \mu_B$/fu derived from the Curie constant C is comparable with the value obtained by Hong *et al* [13] (0.45 μ_B/fu) and is lower than the magnetic moment of the free Ce^{3+} ion (2.4 μ_B). Since the magnetic moment of Ce^{4+} is zero, the reduction of the moment in $CeNi_4B$ may be due to the Ce intermediate-valence state.

The experimental photoemission spectrum of the valence band region of $CeNi_4B$ is shown in figure 1. The valence band spectrum at the Fermi level exhibits the dominance of the Ni(3d) states (1.5 eV). The DOS at the Fermi level in $CeNi_4B$ is reduced in comparison with that for pure Ni and the maximum of the valence band is shifted towards higher energy, from 0.59 eV for pure Ni to 1.5 eV for $CeNi_4B$. We have also experimentally observed the peaks at 17.6 and 20.3 eV, which were identified as arising from $Ce(5p_{3/2})$ and $Ce(5p_{5/2})$, respectively. The XPS valence spectrum is comparable with the results of our calculations of the electronic structure of $CeNi_4B$ (figure 2).

Ab initio calculations show that $CeNi_4B$ is paramagnetic. The energy difference between the total energy of the paramagnetic state and the total energy of the ferromagnetic one is 0.37 meV/atom. The calculated magnetic moment of $CeNi_4B$ is negligible ($10^{-4}\ \mu_B$) in the ferromagnetic state. The total and partial densities of states (DOS) for paramagnetic $CeNi_4B$

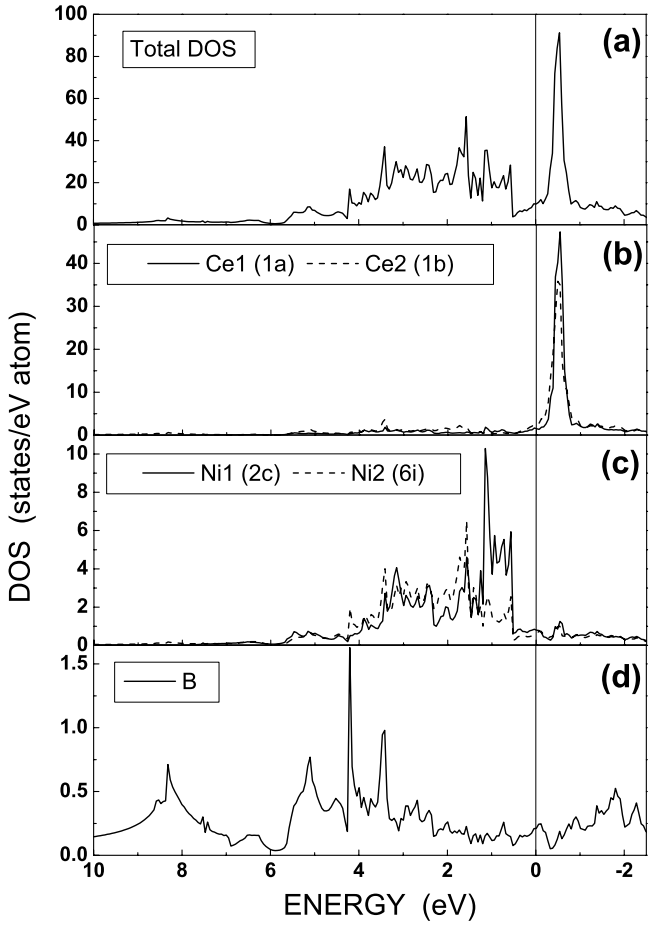

Figure 2. The calculated valence band region of the $CeNi_4B$ compound: (a) the total DOS in states eV^{-1}/cell; (b) the contribution of Ce in sites 1a and 1b; (c) the contribution of Ni atoms in sites 2c and 6i; and (d) the contribution of B atoms.

are displayed in figure 2. The energy scale is presented with respect to the Fermi energy ($E_F = 0$). The total DOS for $CeNi_4B$ consists mostly of the contribution of the Ni atoms in the (2c) and (6i) positions, which contain mainly d states of Ni (below the Fermi level), and the contribution of the f states (above the Fermi energy), which contains mainly f states of Ce atoms in (1a) and (1b) positions. The f peaks of Ce in (1a) and (1b) sites lie at the same energy (0.5 eV), but the peak of Ce in the (1a) position is larger (47.32 states eV^{-1}/atom) than the value of the DOS for the peak of Ce in the (1b) position (35.88 states eV^{-1}/atom). The total and partial DOS exhibit the dominance of the 3d states of Ni below the Fermi energy and reveal the hybridization with 5d states of Ce and 2p states of B over the whole width of the d band of Ni. Hybridization between the f band of Ce and the 3d bands of Ni is observed near the Fermi level. The DOS at the Fermi level is 9.94 states eV^{-1}/cell. There are differences in shape of the partial DOS of the Ni atoms in (2c) and (6i) sites caused by the different types of atom in the nearest neighbourhood. The DOS contribution of the boron atoms (figure 2(d)) is negligible. The electronic specific heat coefficient γ derived from $N(E_F)$ using the relation $\gamma = (\pi k_B)^2 N(E_F)/3$ is about 27.6 mJ K^{-2} mol^{-1}. This value is higher than that of YNi_4B

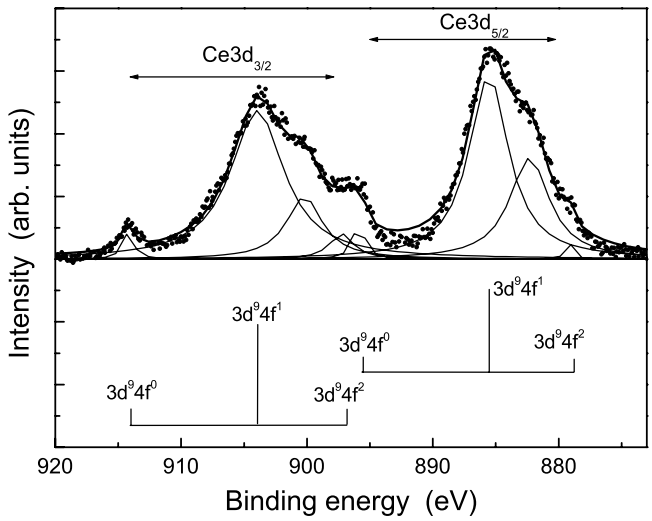

Figure 3. The $3d_{5/2,3/2}$ doublet of the $CeNi_4B$ compound. f^0, f^1 and f^2 stand for the final states related to the main peaks and the satellites. At 900.2 and 882.3 eV, peaks due to oxides are visible.

($\gamma = 14.1$ mJ K^{-2} mol^{-1} [3]) but is significantly lower than in the case of heavy-fermion systems. The theoretical photoemission spectra (figure 1) were obtained by weighting the DOS with appropriate atomic cross-sections for atomic photoemission and applying a convolution with a Lorentzian function, which accounts for a finite experimental resolution ($\sigma = 0.4$ eV in figure 1).

The XPS spectra of the 3d core levels give more information about the 4f configuration and hybridization. The Ce-based intermetallic compounds often show different final states depending on the occupation of the f shell: f^0, f^1 and f^2 [14]. Figure 3 shows the Ce(3d) XPS spectra obtained for $CeNi_4B$. Three final states, f^0, f^1 and f^2, are observed, which exhibit a spin–orbit coupling $\Delta = (3d^94f^1)_{3/2} - (3d^94f^1)_{5/2} = 18.4$ eV. The appearance of the f^0 components is clear evidence of mixed valence. For α-Ce there is also evidence of the $3d^94f^0$ peaks for both $3d_{3/2}$ and $3d_{5/2}$ multiplets, which are not present in γ-Ce [15]; however, the $3d_{5/2}f^0$ peak overlaps with the $3d_{3/2}f^2$ peak and only the $3d_{3/2}f^0$ peak can be accurately estimated [15]. The f occupation in the initial state of α-Ce is connected with the intensity of the $3d^9f^0$ satellite. The XPS of Ce(3d) spectra are usually interpreted in terms of the Gunnarsson–Schönhammer theory [14]. On the basis of this model, the intensity ratios $r_0 = I(f^0)/[I(f^0) + I(f^1) + I(f^2)]$ and $r = I(f^2)/[I(f^1) + I(f^2)]$ are directly related to the f occupation and the hybridization energy Δ, respectively. The separation of the overlapping peaks in the Ce(3d) XPS spectra was carried out on the basis of the Doniach–Šunjić theory [16]. The hybridization energy $\Delta = \pi V \rho_{\max}$ describes the hybridization part of the Anderson impurity Hamiltonian, where $\rho_{\max}$ is the maximum DOS and V is the hybridization matrix element. Assuming dependences of the intensity ratios on the parameters n_f and Δ, as in the case of Ce [14, 15, 17], the Δ value is about 85 meV for the $3d_{3/2}$ band and the f occupancy $n_f \approx 0.83$. The hybridization for α-Ce estimated in this way from XPS 3d spectra [18] is $\Delta = 60$ meV. For Ce intermetallic compounds with strong f-shell instabilities, Δ is of the order of 150 meV [15]. Mixed-valence behaviour was also observed in $CeNi_4B$ employing x-ray absorption near-edge structure (XANES) measurements [19]. It should be emphasized that the estimated values of Δ and n_f can also be affected by the surface effects, which have

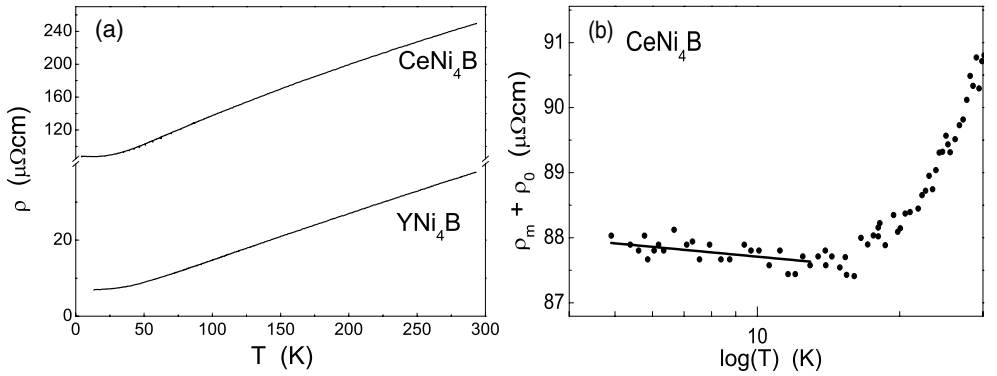

Figure 4. (a) The temperature dependence of the resistivity for $CeNi_4B$ and for the reference (without f electrons) YNi_4B compound. (b) The magnetic part of the $CeNi_4B$ resistivity obtained by subtracting the temperature-dependent part of $\rho(T)$ for YNi_4B.

been precisely extracted for, e.g.: Ce–Rh compounds by comparison of XPS spectra taken with two sources [20]; and $CeIn_3$ and $CeSn_3$ using resonant photoemission spectroscopy [21]. In the case of the presence of a surface contribution, the real bulk hybridization can be even larger, supporting better the general conclusions of this letter.

Figure 4 illustrates the temperature dependence of the electrical resistivity for the $CeNi_4B$ and YNi_4B compounds between 4.2 and 300 K. We conclude that, at low temperatures, Fermi-liquid-type $\rho \sim T^2$ behaviour of $\rho(T)$ is absent. The magnetic contribution $\rho_{\mathrm{mag}}(T)$ (figure 4(b)) is obtained by subtracting the temperature-dependent part of $\rho(T)$ for the non-f-electron reference compound YNi_4B. Below 15 K a shallow minimum typical of the Kondo systems is observed. At low temperature ($T < 12$ K), $\rho_{\mathrm{mag}}(T)$ was analysed in terms of the Kondo theory and the data were fitted with the standard formula $\rho_{\mathrm{mag}}(T) = \rho_0^{\infty} - \rho_{\mathrm{K}} \ln T$ yielding a value of $\rho_0^{\infty} = 88.4\ \mu\Omega$cm for the spin disorder resistivity and $\rho_{\mathrm{K}} = 0.29\ \mu\Omega$cm for the Kondo coefficient. The value of the latter confirms that this effect is very small. It may be induced by a Kondo-like effect originating from the fluctuating Ce valence state.

4. Conclusions

Summarizing the results, one may conclude from both the susceptibility measurements and the XPS spectra that Ce ions in $CeNi_4B$ are in the intermediate-valence state. $CeNi_4B$ is paramagnetic and follows the Curie–Weiss law with $\mu_{\mathrm{eff}} = 0.52\,\mu_{\mathrm{B}}$/fu. However, the effective magnetic moment derived is much lower than the free Ce^{3+}-ion value, equal to 2.54 μ_{B}. Since the magnetic moment of tetravalent cerium is zero, the observed reduction of the magnetic moment can be explained in a natural way by contributions of both $4f^0(Ce^{4+})$ and $4f^1(Ce^{3+})$ configurations.

The electronic structure calculations have also shown that $CeNi_4B$ is paramagnetic. Below the Fermi energy the total DOS contained mainly d states of Ni atoms. The narrow peaks of the f states of Ce atoms were found above the Fermi level. The theoretical calculations of the valence band are in good agreement with the XPS spectrum. The valence band of the x-ray photoemission spectrum is composed mainly of the Ni(3d) band. The values obtained for the f occupancy n_{f} and for the coupling Δ of the f level with the conduction states are consistent with the values known for mixed-valence compounds.

At low temperatures the electrical resistivity reveals a logarithmic slope characteristic of the Kondo-like effect, which may originate from the mixed-valence state.

References

[1] Toliński T, Pugaczowa-Michalska M, Chełkowska G, Szlaferek A and Kowalczyk A 2002 *Phys. Status Solidi* b **231** 446
[2] Hong N M, Thuy N P, Schaudy G, Holubar T, Hilscher G and Franse J J M 1993 *J. Appl. Phys.* **73** 5698
[3] Ravindran P, Sankaralingam S and Asokamani R 1995 *Phys. Rev.* B **52** 12921
[4] Toliński T, Kowalczyk A, Szlaferek A, Timko M and Kovac J 2002 *Solid State Commun.* **122** 363
[5] Toliński T, Chełkowska G and Kowalczyk A 2002 *Solid State Commun.* **122** 145
[6] Toliński T, Kowalczyk A, Szlaferek A, Andrzejewski B, Kovac J and Timko M 2002 *J. Alloys Compounds* **347** 31
[7] Coldea M, Andreica D, Bitu M and Crisan V 1996 *J. Magn. Magn. Mater.* **157/158** 627
[8] Naidyuk N, Reiffers M, Jansen A G M, Yanson I K, Wyder P, Gignoux D and Schmitt D 1993 *Int. J. Mod. Phys.* B **7** 222
[9] Andersen O K, Jepsen O and Sob M 1987 *Electronic Band Structure and its Applications (Springer Lecture Notes in Physics vol 283)* ed M Yussouff (Berlin: Springer) p 1
[10] von Barth U and Hedin L 1972 *J. Phys. C: Solid State Phys.* **5** 1629
[11] Hu C D and Langreth D C 1985 *Phys. Scr.* **32** 391
[12] Jepsen O and Andersen O K 1971 *Solid State Commun.* **9** 1763
[13] Hong N M, Holubar T, Hilscher G, Vybornov M and Rogl P 1994 *IEEE Trans. Magn.* **30** 4966
[14] Gunnarsson O and Schönhammer K 1983 *Phys. Rev.* B **28** 4315
[15] Fuggle J C, Hillebrecht F U, Zolnierek Z, Lässer R, Freiburg Ch, Gunnarsson O and Schönhammer K 1983 *Phys. Rev.* B **27** 7330
[16] Doniach S and Šunjić M 1970 *J. Phys. C: Solid State Phys.* **3** 285
[17] Ślebarski A, Neumann M and Mähl S 1995 *Phys. Rev.* B **51** 11113
[18] Wuilloud E, Moser H R, Schneider W D and Baer Y 1984 *Phys. Rev.* B **38** 7354
[19] Mazumdar C, Hu Z and Kaindl G 1999 *Physica* B **259–261** 89
[20] Braicovich L, Duò L, Vavassori P and Olcese G L 1995 *Surf. Sci.* **331–333** 782
[21] Kim H-D, Tjernberg O, Chiaia G, Kumigashira H, Takahashi T, Duò L, Sakai O, Kasaya M and Lindau I 1995 *Phys. Rev.* B **56** 1620